Published in final edited form as:
J Immunol. 2014 July 1; 193(1): 306–316. doi:10.4049/jimmunol.1400490.

Tetherin promotes the innate and adaptive cell-mediated immune response against retrovirus infection *in vivo*

Sam X. Li, **Bradley S. Barrett**, **Karl J. Heilman**, **Ronald J. Messer**, **Rachel A. Liberatore**, **Paul D. Bieniasz**, **George Kassiotis**, **Kim J. Hasenkrug**, and **Mario L. Santiago**

[*]Department of Medicine, University of Colorado Denver, Aurora, CO 80045, USA

[†]Department of Microbiology, University of Colorado Denver, Aurora, CO 80045, USA

[‖]Department of Immunology, University of Colorado Denver, Aurora, CO 80045, USA

[‡]Rocky Mountain Laboratories, National Institutes of Allergy and Infectious Diseases, NIH, Hamilton, MT 59840 USA

[§]Howard Hughes Medical Institute, Aaron Diamond AIDS Research Center, The Rockefeller University, New York, NY 10016 USA

[¶]Division of Immunoregulation, MRC National Institute for Medical Research, London, United Kingdom

Abstract

Tetherin/BST-2 is a host restriction factor that could directly inhibit retroviral particle release by tethering nascent virions to the plasma membrane. However, the immunological impact of Tetherin during retrovirus infection remains unknown. We now show that Tetherin influences antiretroviral cell-mediated immune responses. In contrast to the direct antiviral effects of Tetherin, which are dependent on cell surface expression, the immunomodulatory effects are linked to the endocytosis of the molecule. Mice encoding endocytosis-competent C57BL/6 Tetherin exhibited lower viremia and pathology at 7 days post-infection with Friend retrovirus (FV) compared to mice encoding endocytosis-defective NZW/LacJ Tetherin. Notably, antiretroviral protection correlated with stronger NK cell responses. In addition, FV infection levels were significantly lower in wild-type C57BL/6 mice than in *Tetherin* knock-out mice at 2 weeks post-infection, and antiretroviral protection correlated with stronger NK cell and virus-specific CD8+ T cell responses. The results demonstrate that Tetherin acts as a modulator of the cell-mediated immune response against retrovirus infection *in vivo.*

Keywords

Tetherin; Bst-2; PDCA-1; H-2; NK cell; Friend retrovirus

Correspondence to: MARIO L. SANTIAGO, PhD Division of Infectious Diseases University of Colorado Denver Phone (303) 724 4946; Fax (303) 724 4926 mario.santiago@ucdenver.edu.

INTRODUCTION

The relationship between host proteins that directly inhibit viruses and the adaptive immune response remains relatively unexplored. One of these 'restriction factors' is Tetherin (also known as BST-2, CD317, HM1.24, and PDCA-1), which is antagonized by the Vpu protein of pandemic HIV-1 strains. In the absence of Vpu, Tetherin blocks virion release by tethering HIV-1 virions to the plasma membrane (1, 2). Due to its potential as a novel HIV-1 drug target, many molecular details governing the Tetherin:Vpu interaction have been elucidated (3). However, despite these advances, it remains unknown whether Tetherin influences the adaptive immune response to retroviruses.

Tetherin is a dimeric Type II membrane protein with an N-terminal cytoplasmic tail, a transmembrane region and a C-terminal glycophosphatidyl inositol anchor (4). Within the short cytoplasmic tail, Tetherin encodes a dual-tyrosine (YxY) motif that is critical for clathrin-mediated endocytosis (5). Cell culture studies revealed that HIV-1 Gag co-localizes with Tetherin in intracellular compartments, suggesting that internalization of Tetherin-bound virions could lead to virion degradation through the endolysosomal pathway (6, 7). It was speculated that virion internalization through Tetherin might have immunological consequences (8), but answering this question is not currently possible using *in vitro* studies and requires *in vivo* experiments not possible in humans. This was exemplified by *in vitro* studies that showed that Tetherin could have both positive (9-11) and negative (1, 2, 12) effects on retrovirus replication. As an approach to test the immunological impact of Tetherin *in vivo*, we have done studies in mouse retrovirus infection models.

We previously reported that a single nucleotide polymorphism (SNP) in mouse *Tetherin* led to an endocytosis defect, resulting in increased levels of cell surface expression (13). An ATG (Methionine) to GTG (Valine) transition in the *Tetherin* start codon of NZW/LacJ (NZW) mice caused the translation of *Tetherin* from a downstream start site, resulting in a truncated Tetherin protein lacking the YxY motif. Interestingly, hybrid (B6 × NZW)F_1 mice, with the genotype *Tetherin*$^{Met/Val}$, had significantly lower Tetherin cell surface expression than NZW mice (*Tetherin*$^{Val/Val}$). This was likely due to the ability of B6:NZW Tetherin heterodimers to be endocytosed with similar efficiency as B6 Tetherin dimers. Thus, the cell surface expression phenotype of B6 *Tetherin* is dominant over NZW *Tetherin in vivo*.

The identification of the NZW *Tetherin* variant provided a unique opportunity to study the impact of Tetherin endocytosis on retroviral infection *in vivo*. We utilized the Friend retrovirus (FV) complex, which causes erythroleukemia in adult immunocompetent mice (14). It is a complex of two retroviruses, a replication-competent but nonpathogenic helper virus called Friend Murine Leukemia Virus (F-MuLV) and a pathogenic, but replication-defective virus called Spleen Focus Forming Virus (SFFV). Earlier FV stocks (until 2008) also contained Lactate Dehydrogenase-elevating Virus (LDV), an endemic mouse RNA virus that exacerbates FV infection (15). Over the last five decades, numerous genetic factors that influence FV resistance and susceptibility have been identified (14). These genes include *Fv1*, which mediates a capsid-dependent post-entry block (16); *Fv2*, a dominant susceptibility gene that dictates splenomegaly induction (17); *H-2*, the murine MHC which

controls adaptive immune responses (18, 19); and *Apobec3/Rfv3*, which influences recovery from viremia by promoting a stronger neutralizing antibody response (20-22).

To evaluate the role of the *Tetherin* endocytosis SNP *in vivo*, we performed a test cross between B6 and NZW mice (Fig. 1A). The test cross utilized [(B6 × NZW)F_1 × NZW]B_1 (or simply, B_1) progeny mice with matched resistance genes and encoding either *Tetherin*$^{Val/Val}$ or *Tetherin*$^{Met/Val}$. Since the FV resistance genes used to classify the B_1 progeny were based on classical genetic studies, we infected mice with LDV+ FV. Using this experimental approach, we found that mice expressing *Tetherin*$^{Val/Val}$ (high surface expression, low endocytosis) exhibited lower levels of acute viremia and disease compared with *Tetherin*$^{Met/Val}$ mice (13). These findings suggested that endocytosis-defective NZW Tetherin was more potent at restricting FV than endocytosis-competent B6 Tetherin *in vivo*. However, this result was puzzling, because with the exception of felids and sheep (23, 24), the YxY motif is evolutionarily conserved across mammalian Tetherins (25, 26), suggesting a strong selective advantage to the host. Thus, the findings raised the issue of why endocytosis-competent Tetherin with apparently weaker direct antiretroviral activity was evolutionarily conserved.

Interestingly, Tetherin-mediated resistance was not observed in the context of *Apobec3/Rfv3* resistance (13). *H-2* genotypes also strongly affect adaptive immunity to FV but we were previously only able to perform experiments in a single *H-2* genotype, *H-2*$^{z/z}$. Thus, it was of interest to determine whether Tetherin impacted virus control in the context of a different *H-2* haplotype. In the first part of the current study, we repeated the B_1 test cross to generate sufficient numbers of mice with the *H-2*$^{b/z}$ genotype to analyze for MHC resistance effects. Surprisingly, we found that the impact of the Tetherin endocytosis SNP on acute FV infection and disease was quite different in the *H-2*$^{b/z}$ haplotype than it was in *H-2*$^{z/z}$ mice. In the second part of the study, we infected B6 WT (*H-2*$^{b/b}$) versus B6 *Tetherin* KO mice with LDV-free FV to ascertain that Tetherin restriction was not solely due to the presence of LDV. The data further highlighted a significant role for B6 Tetherin in inhibiting FV replication, but this protective effect did not appear to be due to direct retrovirus restriction. Rather, our results suggested that Tetherin functioned as a modulator of the antiretroviral cell-mediated immune response.

MATERIALS AND METHODS

Mice

C57BL/6J (B6) and NZW/LacJ (NZW) mice were purchased from the Jackson Laboratory. *Tetherin* KO mice were generated in the B6 genetic background (27). Mice used in this study ranged from 8 to 12 weeks of age. All mice were handled in accordance with the recommendations in the NIH Guide for the Care and Use of Laboratory Animals, and approved by the University of Colorado IACUC Permit Number B-89709(10)1E. Mouse infections were performed under isoflurane anesthesia, and all efforts were made to minimize suffering.

Genetic backcrossing approach

A genetic backcrossing approach (13) was used to generate B_1 progeny mice expressing either endocytosis-defective or endocytosis-competent Tetherin (Fig. 1A) after taking into account 4 major FV resistance genes encoded in different chromosomes relative to *Tetherin*. *Fv1* restriction, which dictates N- versus B-tropism of the virus (16), was offset by infecting B_1 mice with a dual (NB)-tropic strain of FV. The *Fv2* gene controls susceptibility to FV-induced splenomegaly and the susceptibility allele is dominant (17). Thus, backcrossing to NZW guaranteed that all progeny mice harbored the *Fv2* susceptibility allele. *Rfv3* is encoded by *Apobec3*, restricts acute FV replication (20, 28), and promotes recovery from viremia by influencing the neutralizing antibody response. To negate epistatic effects of the resistant form of *Apobec3* (13), only mice genotyped as $Rfv3^{s/s}$ were investigated. Lastly, B_1 progeny were genotyped for $H\text{-}2^{b/z}$ and the *Tetherin* SNP by direct sequencing. $H\text{-}2^{b/z}$ mice were grouped according to their *Tetherin* genotype (Fig. 1A).

H-2, Apobec3, and *Tetherin* genotyping

Mice were genotyped for *H-2*, *Apobec3*, and *Tetherin* as previously described (13). *H-2* was genotyped by direct sequencing of a 1.0 kb *H2-Q1* PCR amplicon, and *Apobec3/Rfv3* was genotyped using a set of 3 primers flanking and positioned within a 530 bp Xenotropic Murine Leukemia Virus (X-MLV) insertion in B6 mice (22). The *Tetherin* SNP was genotyped by amplifying a 582 bp fragment spanning the start codon.

FV infection

B_1 mice were infected with an FV stock containing NB-tropic F-MuLV, SFFV and LDV (13). B6 WT and *Tetherin* KO mice were infected with B-tropic LDV-free FV (F-MuLV and SFFV only) (15, 29). F-MuLV is critical for viral replication, and all the virological assays described here were specific for F-MuLV. The NB-tropic FV stocks used in this study were prepared in BALB/c mice and had equivalent Spleen Focus Forming Unit (SFFU) titers in BALB/c and NZW mice (data not shown). B_1 mice were infected intravenously with 500 SFFU of LDV+ FV, whereas B6 WT and *Tetherin* KO mice were infected intravenously with 10^4 SFFU of LDV-free FV.

Immunophenotyping

Splenocytes were stained with the F-MuLV Env gp70-specific MAb 720 (30) for 1 h, then co-stained with: Ter119-FITC (clone TER-119), CD3-Alexa700 (17A2), (BD Biosciences); either PDCA-1-PE (eBio927) or CD11b-PE (M1/70) (BD Biosciences), CD11c-PE-Cy7 (N418), (eBioscience); CD19-PerCP-Cy5.5 (6D5) (Biolegend) and anti-mouse IgGAllophycocyanin (Columbia Biosciences) for 30 min. A separate aliquot of splenocytes (4×10^6) were treated with RBC lysis buffer (eBioscience) then stimulated with PMA (25 ng/ml) and Ionomycin (0.7 μg/ml) (Sigma), and stained with CD107a-PE-Cy7 (1D4B, BD Biosciences) for 5 h at 37°C and 5% CO_2. The cells were treated with Golgi Plug (BD Biosciences) for the final 4 h of incubation. The cells were then co-stained with CD4-PE-CF594 (RM4-5), CD8α-FITC (53-6.7), and either CD49b-Allophycocyanin (DX5) or NK-1.1-Allophycocyanin (PK136) (BD Biosciences) for 30 min. DX5 was used to identify NK cells in B_1 mice. Although NK1.1 is a more specific NK cell marker, the PK136 MAb

only works for certain strains of mice such as B6. The cells were permeabilized in Perm/Fix buffer, and stained with IFNγ-PE (XMG1.2) (BD Biosciences). An LSR-II flow cytometer (BD Biosciences) was used to capture up to 250,000 events per sample, and Flowjo software (Treestar) was used for data analysis. Isotype controls and were used for gating. To identify FV-infected cells, MAb720 gates were set using splenocytes from an uninfected mouse. FMO and isotype controls also gave similar results based on previous optimization experiments.

Dextramer analysis

RBC-lysed splenocytes (4×10^6) were stained with D^bGagL Dextramer (H-2D^b/Abu-Abu-L-Abu-LTVL-APC) (Immudex) for 10 min, then costained with CD8α-FITC (53-6.7, BD Biosciences) for another 20 min at 4°C in the dark. The cells were washed 3×, fixed in 1% paraformaldehyde, and analyzed in an LSR-II flow cytometer (BD Biosciences) within 2 h. Uninfected splenocytes stained with the D^bGagL Dextramer were used for gating.

Plasma viral load

F-MuLV RNA copy numbers in the plasma were measured by quantitative PCR (22, 31). RNA extracted from 5 μl of plasma was added to 1× One-Step Taqman Reverse Transcriptase-PCR reaction mixture (Applied Biosystems). T7-transcribed RNA standards were used to calculate FV copy numbers.

FV-specific IgG titer

ELISAs were used to measure plasma FV-specific IgG titers (31). Briefly, 96-well plates were coated with intact FV virions. Plasma samples from mice were heat inactivated (56°C for 30 min) and incubated with the antigen. A biotin-conjugated goat anti-mouse antibody and Streptavidin-HRP (Southern Biotech) were used to detect bound FV-specific IgG. The plate was read in a Victor X5 plate reader (Perkin Elmer). Endpoint IgG titers were calculated as the plasma dilution corresponding to 2× the PBS background using best-fit nonlinear regression (GraphPad Prism 5.0).

Statistical analysis

Two-group comparisons were done using 2-tailed unpaired Student's *t* test. For datasets with skewed distribution based on the Kolmogorov-Smirnov normality test ($p<0.05$), a 2-tailed Mann-Whitney U test was performed. Correlation analyses were done using Pearson's *r* (GraphPad Prism 5.0). *P* values less than 0.05 were considered statistically significant.

RESULTS

Lower Tetherin cell surface expression in *Tetherin*$^{Met/Val}$ mice

To investigate the impact of the *Tetherin* endocytosis SNP in B_1 mice, all the major genes influencing FV infection, particularly *Fv1, Fv2, Apobec3/Rfv3* and *H-2* were controlled as previously described (13) (Fig. 1A). We obtained *Rfv3*$^{s/s}$ *H-2*$^{b/z}$ B_1 progeny mice that were genotyped as either *Tetherin*$^{Val/Val}$ (n=10) or *Tetherin*$^{Met/Val}$ (n=9). To be consistent with

the earlier study (13), spleens and plasma samples were harvested at 7 days post infection (dpi) with FV.

We previously reported that *Tetherin*$^{Met/Val}$ mice exhibited lower Tetherin cell surface expression compared to *Tetherin*$^{Val/Val}$ mice, likely due to the expression of endocytosis-competent Tetherin dimers (13). To confirm these phenotypes in *Rfv3*$^{s/s}$ *H-2*$^{b/z}$ B_1 mice, Tetherin expression levels on total and FV-infected splenocytes were examined by flow cytometry (Fig. 1B). FV-infected splenocytes were identified following staining with a monoclonal antibody against the F-MuLV envelope protein, MAb 720 (30). Significantly higher surface Tetherin+ cells were observed in *Tetherin*$^{Val/Val}$ versus *Tetherin*$^{Met/Val}$ total (Fig. 1C) and MAb720+ (Fig. 1D) splenocytes. Similar results were observed using Tetherin mean fluorescence intensity (MFI) values in FV-infected splenocytes, Ter119+ erythroblasts, CD11c+ DCs (Fig. 1E) and CD19+ B cells (data not shown). These data show that in B_1 mice of the *H-2*$^{b/z}$ haplotype, NZW *Tetherin* SNP homozygosity results in significantly increased Tetherin cell surface expression.

Endocytosis-competent Tetherin inhibits acute FV replication and disease in the *H-2*$^{b/z}$ genetic background

A hallmark of FV disease is splenomegaly due to FV-induced proliferation of Ter119+ erythroblasts (17, 32, 33). In contrast to previous studies with *H-2*$^{z/z}$ mice, *H-2*$^{b/z}$ mice expressing *Tetherin*$^{Val/Val}$ had more pathology than *Tetherin*$^{Met/Val}$ mice at 7 dpi with FV, with significantly larger spleens (Fig. 2A) and more absolute numbers of splenic Ter119+ erythroblasts (Fig. 2B). In addition, plasma viral loads as analyzed by quantitative PCR to detect F-MuLV RNA (22, 31) were 10-fold higher in *Tetherin*$^{Val/Val}$ than *Tetherin*$^{Met/Val}$ mice (Fig. 2C). The percentage of surface Tetherin+ splenocytes positively correlated with splenomegaly (Fig. 2D), erythroblast numbers (Fig. 2E), and plasma viral load (Fig. 2F). Thus, in sharp contrast to our previous results in the *H-2*$^{z/z}$ background (13), the endocytosis competent form of Tetherin was protective in the *H-2*$^{b/z}$ haplotype.

Endocytosis-competent Tetherin is associated with a stronger NK cell response in the *H-2*$^{b/z}$ genetic background

In co-transfection experiments, NZW Tetherin was more potent in inhibiting F-MuLV virion release than B6 Tetherin *in vitro* (13). Since NZW *Tetherin* (*Tetherin*$^{Val/Val}$) was less protective in the *H-2*$^{b/z}$ background *in vivo*, we hypothesized that the protective effect of the *Tetherin*$^{Met/Val}$ genotype might be due to mechanisms other than direct restriction. The *H-2* locus encodes the MHC-I and MHC-II proteins that prime CD8+ and CD4+ T cell responses (34) as well as non-classical MHC molecules that direct natural killer (NK) cell responses (35). Thus, we next sought to determine whether the protective effect of endocytosis-competent Tetherin in *H-2*$^{b/z}$ mice correlated with cell-mediated immune responses.

Splenocytes at 7 dpi were stimulated for 5 h *ex vivo* with PMA and Ionomycin and then stained for T cell markers CD4 and CD8, a ‘pan-NK’ marker, DX5 (CD49b), surface CD107a (a marker of degranulation) and intracellular IFNγ (Fig. 3A). Since some T cell subsets express DX5 (36, 37), we classified NK cells as DX5+CD4-CD8-. Given the significant difference in spleen mass between *Tetherin*$^{Val/Val}$ and *Tetherin*$^{Met/Val}$ mice (Fig.

2A), we first checked the absolute numbers of NK, CD4+ T and CD8+ T cells, and found no significant differences between the two cohorts (Supplementary Fig. 1A to 1C). Thus, subsequent analyses of IFNγ and CD107a expression were normalized to similar numbers of these immune cells. Surprisingly, antiviral protection correlated strongly with NK cell responses. A significantly higher percentage of NK cells from the spleens of *Tetherin*$^{Met/Val}$ mice were IFNγ+ (Fig. 3B). However, no difference in the percentage of CD107a+ NK cells was observed between *Tetherin*$^{Val/Val}$ and *Tetherin*$^{Met/Val}$ mice ($p>0.05$, data not shown). The percentage of IFNγ+ NK cells had a strong inverse correlation with plasma viral load (Fig. 3C). Importantly, the percentage of IFNγ+ NK cells inversely correlated with surface Tetherin+ splenocytes (Fig. 3D). Similar results were observed using absolute cell numbers (Supplementary Fig. 1D to 1F). These results suggested a link between Tetherin endocytosis and NK cell IFNγ production that mediated protection against acute FV replication. We did not observe a significant impact of the *Tetherin* SNP on CD4+ and CD8+ T cell responses at 7 dpi. CD4+ and CD8+ IFNγ production were similar between *Tetherin*$^{Val/Val}$ and *Tetherin*$^{Met/Val}$ mice (Figs. 3E and 3F, respectively; Supplementary Fig. 1G and 1H). Moreover, no difference in surface CD107a expression on CD8+ T cells or FV-reactive IgG endpoint titers were observed ($p>0.05$, data not shown).

Tetherin expression is induced following FV infection independent of LDV co-infection

The results of the experiments with B_1 mice indicated that endocytosis-competent *Tetherin* influenced innate cellular immunity. As mentioned earlier, these experiments required LDV + FV. LDV could potently stimulate IFNα production (38), and removal of LDV in the FV/LDV stocks reduced IFNα upregulation at 18 to 24 h post-infection (38, 39). Since Type I IFNs could significantly induce Tetherin expression (27, 40), it is possible that LDV co-infection may have primed the host to express unusually high levels of Tetherin (38, 39).

Due to lower levels of IFNα induction, it is possible that LDV-free FV infection may not stimulate the expression of antiretroviral factors. However, we recently showed that independent of LDV co-infection, FV infection of B6 WT mice significantly induced Oligoadenylate Synthetase 1, a canonical type I IFN-inducible gene (41). We therefore tested if LDV-free FV infection could upregulate Tetherin levels. B6 WT mice were infected with FV with or without LDV and Tetherin expression levels were evaluated by flow cytometry (Fig. 4A). As shown in Fig. 4B, FV infection alone significantly induced Tetherin expression in the spleen and the bone marrow to nearly to the same levels as LDV+ FV infection. Thus, LDV was not required to significantly induce Tetherin expression in the FV infection model.

Tetherin promotes the cell-mediated immune response against FV infection

Endocytosis-competent Tetherin did not influence T cell responses in the B_1 cohort, possibly because 7 dpi may be too early to detect potent T cell responses (42, 43). Since LDV-free FV can significantly induce Tetherin expression, B6 WT (n=16) and B6 *Tetherin* KO (n=15) mice were infected with 10^4 SFFU of LDV-free FV, and samples were harvested at 14 dpi. Splenocytes were stimulated for 5 h with PMA and Ionomycin, then stained for CD4 and CD8, the NK cell marker NK1.1, surface CD107a and intracellular IFNγ. Since B6 mice are *Fv2*-resistant, severe splenomegaly was not observed, and B6 WT and B6 *Tetherin*

KO mice had no significant difference in spleen mass, as well as the absolute numbers of Ter119+ erythroblasts, NK cells, CD4+ T cells and CD8+ T cells (Supplementary Fig. 2). However, *Tetherin* KO mice exhibited significantly lower IFNγ production in NK cells, CD8+ T cells and CD4+ T cells (Fig. 5A, 5B and 5C, respectively). Additionally, *Tetherin* KO mice had significantly lower percentages of CD107a+ NK and CD8+ T cells (Fig. 5D and 5E). Statistically-significant differences were also observed using absolute numbers (data not shown). In contrast, FV-specific IgG titers were not significantly different between WT and *Tetherin* KO mice (Fig. 5F).

To determine whether Tetherin promoted the virus-specific CD8+ T cell response, we stained unstimulated splenocytes for CD8 and a dextramer presenting the immunodominant H-2D^b restricted FV epitope from the leader region of the alternatively transcribed Glyco-Gag (GagL) protein (44, 45). D^{b}GagL Dextramer+ cells were gated according to a stained, uninfected sample (Fig. 6A). At 14 dpi, *Tetherin* KO mice had a significantly lower percentage of D^{b}GagL-specific CD8+ T cells compared with WT mice (Fig 6B). Altogether, these data demonstrate that at 14 dpi, B6 Tetherin augments the NK cell, CD4+ T cell and CD8+ T cell response against FV infection *in vivo*.

B6 *Tetherin* is associated with better immune control of FV replication

To determine if the differences in cell-mediated immune response were relevant *in vivo*, we evaluated whether B6 *Tetherin* had an impact on FV infection. Cellular FV infection levels were quantified in WT and *Tetherin* KO spleens at 14 dpi by flow cytometry. Splenocytes from *Tetherin* KO mice had significantly higher FV infection (Fig. 7A), particularly in CD19+ B cells (Fig. 7B). Interestingly, splenocyte infection levels inversely correlated with CD107a expression in CD8+ T cells (Fig. 7C), and more specifically, D^{b}GagL+ CD8+ T cells (Fig. 7D). No correlation between splenocyte FV infection levels was observed for IFNγ expression in NK cells, CD4+ T cells or CD8+ T cells (p>0.05; data not shown).

Plasma samples were evaluated for F-MuLV RNA copies by qPCR. These analyses revealed that *Tetherin* KO mice had significantly higher plasma viral loads compared to WT mice (Fig. 8A). Viral loads inversely correlated with IFNγ production and cytolytic activity by NK cells (Fig. 8B and 8C) and with levels of virus-specific CD8+ T cells (D^{b}GagL+) (Fig. 8D), but not with IFNγ expression by CD8+ or CD4+ T cells (p>0.05; data not shown). Thus, viral inhibition by B6 Tetherin is associated with enhanced CD8+ T cell and NK cell responses.

DISCUSSION

To address a critical knowledge gap on the immunological impact of *Tetherin* in retrovirus infection, we utilized two *in vivo* approaches using the FV infection model. First, we probed the role of a *Tetherin* SNP that resulted in an endocytosis defect in NZW but not B6 mice through a classical genetic backcrossing approach (13). In a previous study, we found that in *H-2*$^{z/z}$ mice, endocytosis-defective NZW Tetherin was more protective. This result was consistent with *in vitro* co-transfection studies showing that NZW Tetherin more potently inhibited F-MuLV virion release than B6 Tetherin (13). Thus, the results with *H-2*$^{z/z}$ mice likely reflect the direct antiretroviral activity of Tetherin. Suprisingly, in *H-2*$^{b/z}$ mice, we

obtained the opposite result: endocytosis-competent Tetherin was more protective. Counterintuitively, low Tetherin cell surface expression correlated with higher protection from FV infection and disease. Since the *H-2*^{b} allele is associated with stronger CD4+ and CD8+ T cell responses against FV infection (14, 46-48), we initially hypothesized a T cell component. However, the strongest correlate of protection was the NK cell response. NK cells can significantly protect mice during acute FV infection based on NK cell depletion strategies (49-53). In follow-up work, similar depletion strategies should help determine the relative contribution of NK cells (versus T cells) in B6 Tetherin-mediated antiviral protection in B_1 mice.

CD8+ and CD4+ T cell responses are critical for recovery from FV infection (33, 42, 43, 54, 55) and these T cell responses peak shortly after 7 dpi (56, 57). Thus, the relatively weak association between Tetherin and T cell responses in the B_1 experiments led us to perform a second set of studies, this time with B6 WT and B6 *Tetherin* KO mice at 14 dpi. Since LDV co-infection could alter adaptive immune responses to FV (15, 29, 38, 39, 58), and the experimental design was not constrained by genetic parameters defined by classical FV infection studies (in contrast to the B_1 study), we utilized LDV-free FV stocks. Further strengthening the role of Tetherin as an antiretroviral factor *in vivo*, we observed significantly higher FV infection levels in *Tetherin* KO mice. Moreover, we observed significantly lower NK cell, CD4+ T cell and CD8+ T cell responses but normal FV-specific IgG titers in B6 *Tetherin* KO mice. Importantly, NK cell and virus-specific CD8+ T cell responses inversely correlated with cellular FV infection levels and viremia, consistent with a prominent role for these cellular immune responses in early acute infection. These findings imply that improved retroviral control was not due to direct Tetherin-mediated restriction, but was due to stronger cell-mediated immune responses.

The results of the B_1 study link the ability of B6 *Tetherin* to enhance NK cell responses to its endocytic function. NK cells are highly responsive to Type I IFN stimulation through intrinsic IFNα receptor expression (51). Plasmacytoid DCs (pDCs), which produce the highest levels of Type I IFNs on a per-cell basis *in vivo*, sense retroviruses through endosomal Toll-like Receptor 7 (TLR7) (59), express Tetherin (60), and may regulate NK cell responses in a virus-dependent manner (61). In fact, the other name for Tetherin is Plasmacytoid Dendritic Cell Antigen-1 (60), a marker used to distinguish pDCs. Thus, Tetherin-mediated endocytosis of virions in pDCs may augment endosomal TLR7 stimulation, resulting in increased Type I IFN production to stimulate NK cell activity. Consistent with this notion, WT 129/SvJ pDCs produced higher levels of IFNα following stimulation with Murine Cytomegalovirus (MCMV) than 129/SvJ *Tetherin* KO pDCs *ex vivo* (62). We are in the process of backcrossing the NZW *Tetherin* SNP into the B6 genetic background to allow for systematic comparisons of antiretroviral NK cell responses between congenic mice expressing B6, NZW or null Tetherin.

An endocytosis-dependent model can also be invoked to explain how B6 Tetherin influenced T cell responses. It has been suggested that peptide levels may be a limiting factor in MHC-antigen presentation (63). We hypothesize that Tetherin-mediated re-uptake of virions into endosomes may increase the viral peptide pool, resulting in higher density of MHC-II-viral peptide complexes. The significant impact of B6 Tetherin on CD8+ T cell

responses also suggests that Tetherin endocytosis may enhance cross-presentation of viral peptides to MHC-I. Tracking the fate of virions and viral peptide-MHC complexes in antigen-presenting cells expressing endocytosis-competent versus endocytosis-defective Tetherin would be a powerful means to test this model in follow-up work. Interestingly, 129/SvJ *Tetherin* knock-out mice infected with vesicular stomatitis virus and influenza B virus exhibited stronger CD8+ T cell responses in the lungs than 129/SvJ WT mice (62). Thus, Tetherin appears to differentially modulate cell-mediated immunity against retroviruses and negative-stranded RNA viruses *in vivo*. Further studies should determine if Tetherin could promote cell-mediated immunity against other nonretroviral pathogens.

Recently, human Tetherin was shown to activate NF-κB (64-66), a central regulator of adaptive immunity (67). The functional determinants mapped to the cytoplasmic tail, and the YxY motif served as a critical interface for interaction with the adaptors TAK1 and TRAF6 (64-66). However, this signaling property appears to be specific to human Tetherin, since mouse and monkey Tetherins did not exhibit NF-κB signaling activity (64). It remains to be determined whether B6 Tetherin may have other signaling properties that map to its cytoplasmic tail that may alternatively explain its impact on cell-mediated immunity.

In conclusion, our findings provide evidence that Tetherin does not just function as a retrovirus restriction factor, but also functions to promote the antiretroviral cell-mediated immune response. We ascribe this immunomodulatory role to Tetherin's cytoplasmic tail that encompass a highly conserved endocytosis motif, which influenced virus infection in an *H-2* dependent manner. These findings could have important implications for HIV-1 infection, since human *Tetherin* mRNA harbors a leaky Kozak sequence that results in the translation of a full length (B6-like) and a truncated (NZW-like) Tetherin protein (66). Thus, modulating the magnitude and balance between these two alternative forms of human Tetherin in accordance with an individual's MHC-resistance profile may have biomedical implications. Finally, NK cell, CD4+ T cell and CD8+ T cell responses have the potential to inhibit HIV-1 (68), but if the magnitude or breadth of the response is not strong enough, the virus escapes. The findings presented here provide a strong rationale to investigate the impact of human Tetherin and inhibitors of the Vpu:Tetherin interaction in strengthening CD8+ T cell, CD4+ T cell and NK cell responses against HIV-1 infection.

Supplementary Material

Refer to Web version on PubMed Central for supplementary material.

Acknowledgments

We thank K. Gibbert and U. Dittmer (University of Duisberg-Essen) for sharing NK cell data prior to publication. We also thank T. Morrison, D. Barton, C. Jakubzick, J. D. Beckham, C. Wilson, S. Dillon and members of the Santiago Laboratory (University of Colorado Denver) for helpful advice and discussions.

Funding support: National Institutes of Health (NIH) R01 AI090795 (M.L.S.), the Colorado Clinical and Translational Sciences Institute TL1 TR000155 (S.X.L.), Molecular Pathogenesis of Infectious Disease T32 AI052066 (S.X.L.), The Howard Hughes Medical Institute (P.D.B.), the NIH Division of Intramural Research (K.J.Ha) and the UCD Department of Medicine Early Career Scholar Program (M.L.S.).

REFERENCES

1. Neil SJ, Zang T, Bieniasz PD. Tetherin inhibits retrovirus release and is antagonized by HIV-1 Vpu. Nature. 2008; 451:425–430. [PubMed: 18200009]
2. Van Damme N, Goff D, Katsura C, Jorgenson RL, Mitchell R, Johnson MC, Stephens EB, Guatelli J. The interferon-induced protein BST-2 restricts HIV-1 release and is downregulated from the cell surface by the viral Vpu protein. Cell Host & Microbe. 2008; 3:245–252. [PubMed: 18342597]
3. Malim MH, Bieniasz PD. HIV restriction factors and mechanisms of evasion. Cold Spring Harb Perspect Med. 2012; 2:a006940. [PubMed: 22553496]
4. Perez-Caballero D, Zang T, Ebrahimi A, McNatt MW, Gregory DA, Johnson MC, Bieniasz PD. Tetherin inhibits HIV-1 release by directly tethering virions to cells. Cell. 2009; 139:499–511. [PubMed: 19879838]
5. Rollason R, Korolchuk V, Hamilton C, Schu P, Banting G. Clathrin-mediated endocytosis of a lipid-raft-associated protein is mediated through a dual tyrosine motif. J Cell Si. 2007; 120:3850–3858.
6. Neil SJ, Eastman SW, Jouvenet N, Bieniasz PD. HIV-1 Vpu promotes release and prevents endocytosis of nascent retrovirus particles from the plasma membrane. PLoS Pathog. 2006; 2:e39. [PubMed: 16699598]
7. Miyakawa K, Ryo A, Murakami T, Ohba K, Yamaoka S, Fukuda M, Guatelli J, Yamamoto N. BCA2/Rabring7 promotes tetherin-dependent HIV-1 restriction. PLoS Pathog. 2009; 5:e1000700. [PubMed: 20019814]
8. Tokarev A, Skasko M, Fitzpatrick K, Guatelli J. Antiviral activity of the interferon-induced cellular protein BST-2/tetherin. AIDS Res Hum Retroviruses. 2009; 25:1197–1210. [PubMed: 19929170]
9. Dietrich I, McMonagle EL, Petit SJ, Vijayakrishnan S, Logan N, Chan CN, Towers GJ, Hosie MJ, Willett BJ. Feline tetherin efficiently restricts release of Feline Immunodeficiency Virus but not spreading of infection. J Virol. 2011; 85:5840–5852. [PubMed: 21490095]
10. Pais-Correia AM, Sachse M, Guadagnini S, Robbiati V, Lasserre R, Gessain A, Gout O, Alcover A, Thoulouze MI. Biofilm-like extracellular viral assemblies mediate HTLV-1 cell-to-cell transmission at virological synapses. Nat Med. 2010; 16:83–89. [PubMed: 20023636]
11. Andrew A, Strebel K. The interferon-inducible host factor bone marrow stromal antigen 2/tetherin restricts virion release, but is it actually a viral restriction factor? J Interferon Cytokine Res. 2011; 31:137–144. [PubMed: 21166593]
12. Casartelli N, Sourisseau M, Feldmann J, Guivel-Benhassine F, Mallet A, Marcelin AG, Guatelli J, Schwartz O. Tetherin restricts productive HIV-1 cell-to-cell transmission. PLoS Pathog. 2010; 6:e1000955. [PubMed: 20585562]
13. Barrett BS, Smith DS, Li SX, Guo K, Hasenkrug KJ, Santiago ML. A single nucleotide polymorphism in *Tetherin* promotes retrovirus restriction *in vivo*. PLoS Pathog. 2012; 8:e1002596. [PubMed: 22457621]
14. Hasenkrug KJ, Chesebro B. Immunity to retroviral infection: the Friend virus model. Proc Natl Acad Sci U S A. 1997; 94:7811–7816. [PubMed: 9223268]
15. Robertson SJ, Ammann CG, Messer RJ, Carmody AB, Myers L, Dittmer U, Nair S, Gerlach N, Evans LH, Cafruny WA, Hasenkrug KJ. Suppression of acute anti-friend virus CD8+ T-cell responses by coinfection with Lactate Dehydrogenase-elevating Virus. J Virol. 2008; 82:408–418. [PubMed: 17959678]
16. Best S, Tissier P. Le, Towers G, Stoye JP. Positional cloning of the mouse retrovirus restriction gene *Fv1*. Nature. 1996; 382:826–829. [PubMed: 8752279]
17. Persons DA, Paulson RF, Loyd MR, Herley MT, Bodner SM, Bernstein A, Correll PH, Ney PA. *Fv2* encodes a truncated form of the Stk receptor tyrosine kinase. Nat Genet. 1999; 23:159–165. [PubMed: 10508511]
18. Britt WJ, Chesebro B. *H-2D* (*Rfv-1*) gene influence on recovery from Friend virus leukemia is mediated by nonleukemic cells of the spleen and bone marrow. J Exp Med. 1980; 152:1795–1804. [PubMed: 6935387]
19. Chesebro B, Wehrly K. *Rfv-1* and *Rfv-2*, two *H-2*-associated genes that influence recovery from Friend leukemia virus-induced splenomegaly. J Immunol. 1978; 120:1081–1085. [PubMed: 641338]

20. Santiago ML, Montano M, Benitez R, Messer RJ, Yonemoto W, Chesebro B, Hasenkrug KJ, Greene WC. *Apobec3* encodes *Rfv3*, a gene influencing neutralizing antibody control of retrovirus infection. Science. 2008; 321:1343–1346. [PubMed: 18772436]
21. Tsuji-Kawahara S, Chikaishi T, Takeda E, Kato M, Kinoshita S, Kajiwara E, Takamura S, Miyazawa M. Persistence of viremia and production of neutralizing antibodies differentially regulated by polymorphic *APOBEC3* and *BAFF-R* loci in Friend virus-infected mice. J Virol. 2010; 84:6082–6095. [PubMed: 20375169]
22. Santiago ML, Smith DS, Barrett BS, Montano M, Benitez RL, Pelanda R, Hasenkrug KJ, Greene WC. Persistent Friend virus replication and disease in *Apobec3*-deficient mice expressing functional B-cell-activating factor receptor. J Virol. 2011; 85:189–199. [PubMed: 20980520]
23. Celestino M, Calistri A, Del Vecchio C, Salata C, Chiuppesi F, Pistello M, Borsetti A, Palu G, Parolin C. Feline tetherin is characterized by a short N-terminal region and is counteracted by the Feline Immunodeficiency Virus envelope glycoprotein. J Virol. 2012; 86:6688–6700. [PubMed: 22514338]
24. Arnaud F, Black SG, Murphy L, Griffiths DJ, Neil SJ, Spencer TE, Palmarini M. Interplay between ovine bone marrow stromal cell antigen 2/tetherin and endogenous retroviruses. J Virol. 2010; 84:4415–4425. [PubMed: 20181686]
25. Lim ES, Malik HS, Emerman M. Ancient adaptive evolution of tetherin shaped the functions of Vpu and Nef in human immunodeficiency virus and primate lentiviruses. J Virol. 2010; 84:7124–7134. [PubMed: 20444900]
26. Liu J, Chen K, Wang JH, Zhang C. Molecular evolution of the primate antiviral restriction factor tetherin. PLoS One. 2010; 5:e11904. [PubMed: 20689591]
27. Liberatore RA, Bieniasz PD. Tetherin is a key effector of the antiretroviral activity of type I interferon *in vitro* and *in vivo*. Proc Natl Acad Sci U S A. 2011; 108:18097–18101. [PubMed: 22025715]
28. Takeda E, Tsuji-Kawahara S, Sakamoto M, Langlois MA, Neuberger MS, Rada C, Miyazawa M. Mouse APOBEC3 restricts Friend leukemia virus infection and pathogenesis *in vivo*. J Virol. 2008; 82:10998–11008. [PubMed: 18786991]
29. Marques R, Antunes I, Eksmond U, Stoye J, Hasenkrug K, Kassiotis G. B lymphocyte activation by coinfection prevents immune control of Friend virus infection. J Immunol. 2008; 181:3432–3440. [PubMed: 18714015]
30. Robertson MN, Miyazawa M, Mori S, Caughey B, Evans LH, Hayes SF, Chesebro B. Production of monoclonal antibodies reactive with a denatured form of the Friend murine leukemia virus gp70 envelope protein: use in a focal infectivity assay, immunohistochemical studies, electron microscopy and western blotting. J Virol Methods. 1991; 34:255–271. [PubMed: 1744218]
31. Smith DS, Guo K, Barrett BS, Heilman KJ, Evans LH, Hasenkrug KJ, Greene WC, Santiago ML. Noninfectious retrovirus particles drive the APOBEC3/Rfv3 dependent neutralizing antibody response. PLoS Pathog. 2011; 7:e1002284. [PubMed: 21998583]
32. Li JP, D'Andrea AD, Lodish HF, Baltimore D. Activation of cell growth by binding of Friend spleen focus-forming virus gp55 glycoprotein to the erythropoietin receptor. Nature. 1990; 343:762–764. [PubMed: 2154701]
33. Dittmer U, Race B, Peterson KE, Stromnes IM, Messer RJ, Hasenkrug KJ. Essential roles for CD8+ T cells and gamma interferon in protection of mice against retrovirus-induced immunosuppression. J Virol. 2002; 76:450–454. [PubMed: 11739713]
34. Neefjes J, Jongsma ML, Paul P, Bakke O. Towards a systems understanding of MHC class I and MHC class II antigen presentation. Nat Rev Immunol. 2011; 11:823–836. [PubMed: 22076556]
35. Thielens A, Vivier E, Romagne F. NK cell MHC class I specific receptors (KIR): from biology to clinical intervention. Curr Opin Immunol. 2012; 24:239–245. [PubMed: 22264929]
36. Kassiotis G, Gray D, Kiafard Z, Zwirner J, Stockinger B. Functional specialization of memory Th cells revealed by expression of integrin CD49b. J Immunol. 2006; 177:968–975. [PubMed: 16818752]
37. Slifka MK, Pagarigan RR, Whitton JL. NK markers are expressed on a high percentage of virus-specific CD8+ and CD4+ T cells. J Immunol. 2000; 164:2009–2015. [PubMed: 10657652]

38. Ammann CG, Messer RJ, Peterson KE, Hasenkrug KJ. Lactate dehydrogenase-elevating virus induces systemic lymphocyte activation via TLR7-dependent IFNalpha responses by plasmacytoid dendritic cells. PLoS One. 2009; 4:e6105. [PubMed: 19568424]
39. Gerlach N, Schimmer S, Weiss S, Kalinke U, Dittmer U. Effects of Type I Interferons on Friend retrovirus infection [Author's correction]. J Virol. 2007; 81:6160.
40. Harper MS, Barrett BS, Smith DS, Li SX, Gibbert K, Dittmer U, Hasenkrug KJ, Santiago ML. IFN-alpha treatment inhibits acute Friend retrovirus replication primarily through the antiviral effector molecule Apobec3. J Immunol. 2013; 190:1583–1590. [PubMed: 23315078]
41. Li SX, Barrett BS, Harper MS, Heilman KJ, Halemano K, Steele AK, Guo K, Silverman RH, Santiago ML. Ribonuclease L is not critical for innate restriction and adaptive immunity against Friend retrovirus infection. Virology. 2013; 443:134–142. [PubMed: 23725696]
42. Hasenkrug KJ. Lymphocyte deficiencies increase susceptibility to friend virus-induced erythroleukemia in *Fv-2* genetically resistant mice. J Virol. 1999; 73:6468–6473. [PubMed: 10400741]
43. Pike R, Filby A, Ploquin MJ, Eksmond U, Marques R, Antunes I, Hasenkrug K, Kassiotis G. Race between retroviral spread and CD4+ T-cell response determines the outcome of acute Friend virus infection. J Virol. 2009; 83:11211–11222. [PubMed: 19692462]
44. Dittmer U, He H, Messer RJ, Schimmer S, Olbrich AR, Ohlen C, Greenberg PD, Stromnes IM, Iwashiro M, Sakaguchi S, Evans LH, Peterson KE, Yang G, Hasenkrug KJ. Functional impairment of CD8(+) T cells by regulatory T cells during persistent retroviral infection. Immunity. 2004; 20:293–303. [PubMed: 15030773]
45. Chen W, Qin H, Chesebro B, Cheever MA. Identification of a gag-encoded cytotoxic T-lymphocyte epitope from FBL-3 leukemia shared by Friend, Moloney, and Rauscher murine leukemia virus-induced tumors. J Virol. 1996; 70:7773–7782. [PubMed: 8892898]
46. Peterson KE, Iwashiro M, Hasenkrug KJ, Chesebro B. Major histocompatibility complex class I gene controls the generation of gamma interferon-producing CD4(+) and CD8(+) T cells important for recovery from friend retrovirus-induced leukemia. J Virol. 2000; 74:5363–5367. [PubMed: 10799615]
47. Miyazawa M, Nishio J, Wehrly K, Chesebro B. Influence of MHC genes on spontaneous recovery from Friend retrovirus-induced leukemia. J Immunol. 1992; 148:644–647. [PubMed: 1729380]
48. Hasenkrug KJ, Sprangrude GJ, Nishio J, Brooks DM, Chesebro B. Recovery from Friend disease in mice with reduced major histocompatibility complex class I expression. J Virol. 1994; 68:2059–2064. [PubMed: 8138991]
49. Francois S, Peng J, Schwarz T, Duppach J, Gibbert K, Dittmer U, Kraft AR. NK cells improve control of Friend virus infection in mice persistently infected with murine cytomegalovirus. Retrovirology. 2013; 10:58. [PubMed: 23738889]
50. Littwitz E, Francois S, Dittmer U, Gibbert K. Distinct roles of NK cells in viral immunity during different phases of acute Friend retrovirus infection. Retrovirology. 2013; 10:127. [PubMed: 24182203]
51. Gibbert K, Joedicke JJ, Meryk A, Trilling M, Francois S, Duppach J, Kraft A, Lang KS, Dittmer U. Interferon-alpha subtype 11 activates NK cells and enables control of retroviral infection. PLoS Pathog. 2012; 8:e1002868. [PubMed: 22912583]
52. Ogawa T, Tsuji-Kawahara S, Yuasa T, Kinoshita S, Chikaishi T, Takamura S, Matsumura H, Seya T, Saga T, Miyazawa M. Natural killer cells recognize Friend retrovirus-infected erythroid progenitor cells through NKG2D-RAE-1 interactions *in vivo*. J Virol. 2011; 85:5423–5435. [PubMed: 21411527]
53. Iwanami N, Niwa A, Yasutomi Y, Tabata N, Miyazawa M. Role of natural killer cells in resistance against Friend retrovirus-induced leukemia. J Virol. 2001; 75:3152–3163. [PubMed: 11238842]
54. Hasenkrug KJ, Brooks DM, Dittmer U. Critical role for CD4(+) T cells in controlling retrovirus replication and spread in persistently infected mice. J Virol. 1998; 72:6559–6564. [PubMed: 9658100]
55. Zelinskyy G, Myers L, Dietze KK, Gibbert K, Roggendorf M, Liu J, Lu M, Kraft AR, Teichgraber V, Hasenkrug KJ, Dittmer U. Virus-specific CD8+ T cells upregulate programmed death-1

expression during acute Friend retrovirus infection but are highly cytotoxic and control virus replication. J Immunol. 2011; 187:3730–3737. [PubMed: 21873525]

56. Zelinskyy G, Kraft AR, Schimmer S, Arndt T, Dittmer U. Kinetics of CD8+ effector T cell responses and induced CD4+ regulatory T cell responses during Friend retrovirus infection. Eur J Immunol. 2006; 36:2658–2670. [PubMed: 16981182]
57. Nair SR, Zelinskyy G, Schimmer S, Gerlach N, Kassiotis G, Dittmer U. Mechanisms of control of acute Friend virus infection by CD4+ T helper cells and their functional impairment by regulatory T cells. J Gen Virol. 2010; 91:440–451. [PubMed: 19828756]
58. Duley AK, Ploquin MJ, Eksmond U, Ammann CG, Messer RJ, Myers L, Hasenkrug KJ, Kassiotis G. Negative impact of IFN-gamma on early host immune responses to retroviral infection. J Immunol. 2012; 189:2521–2529. [PubMed: 22821964]
59. Lepelley A, Louis S, Sourisseau M, Law HK, Pothlichet J, Schilte C, Chaperot L, Plumas J, Randall RE, Si-Tahar M, Mammano F, Albert ML, Schwartz O. Innate sensing of HIV-infected cells. PLoS Pathog. 2011; 7:e1001284. [PubMed: 21379343]
60. Blasius AL, Giurisato E, Cella M, Schreiber RD, Shaw AS, Colonna M. Bone marrow stromal cell antigen 2 is a specific marker of type I IFN-producing cells in the naive mouse, but a promiscuous cell surface antigen following IFN stimulation. J Immunol. 2006; 177:3260–3265. [PubMed: 16920966]
61. Swiecki M, Gilfillan S, Vermi W, Wang Y, Colonna M. Plasmacytoid dendritic cell ablation impacts early interferon responses and antiviral NK and CD8(+) T cell accrual. Immunity. 2010; 33:955–966. [PubMed: 21130004]
62. Swiecki M, Wang Y, Gilfillan S, Lenschow DJ, Colonna M. Cutting edge: paradoxical roles of BST2/tetherin in promoting type I IFN response and viral infection. J Immunol. 2012; 188:2488–2492. [PubMed: 22327075]
63. Reits E, Griekspoor A, Neijssen J, Groothuis T, Jalink K, van Veelen P, Janssen H, Calafat J, Drijfhout JW, Neefjes J. Peptide diffusion, protection, and degradation in nuclear and cytoplasmic compartments before antigen presentation by MHC class I. Immunity. 2003; 18:97–108. [PubMed: 12530979]
64. Galao RP, Tortorec A. Le, Pickering S, Kueck T, Neil SJ. Innate sensing of HIV-1 assembly by Tetherin induces NFkappaB-dependent proinflammatory responses. Cell Host & Microbe. 2012; 12:633–644. [PubMed: 23159053]
65. Tokarev A, Suarez M, Kwan W, Fitzpatrick K, Singh R, Guatelli J. Stimulation of NF-kappaB activity by the HIV restriction factor BST2. J Virol. 2013; 87:2046–057. [PubMed: 23221546]
66. Cocka LJ, Bates P. Identification of alternatively translated Tetherin isoforms with differing antiviral and signaling activities. PLoS Pathog. 2012; 8:e1002931. [PubMed: 23028328]
67. Oh H, Ghosh S. NF-kappaB: roles and regulation in different CD4(+) T-cell subsets. Immunol Rev. 2013; 252:41–51. [PubMed: 23405894]
68. Walker BD, Yu XG. Unravelling the mechanisms of durable control of HIV-1. Nat Rev Immunol. 2013; 13:487–498. [PubMed: 23797064]

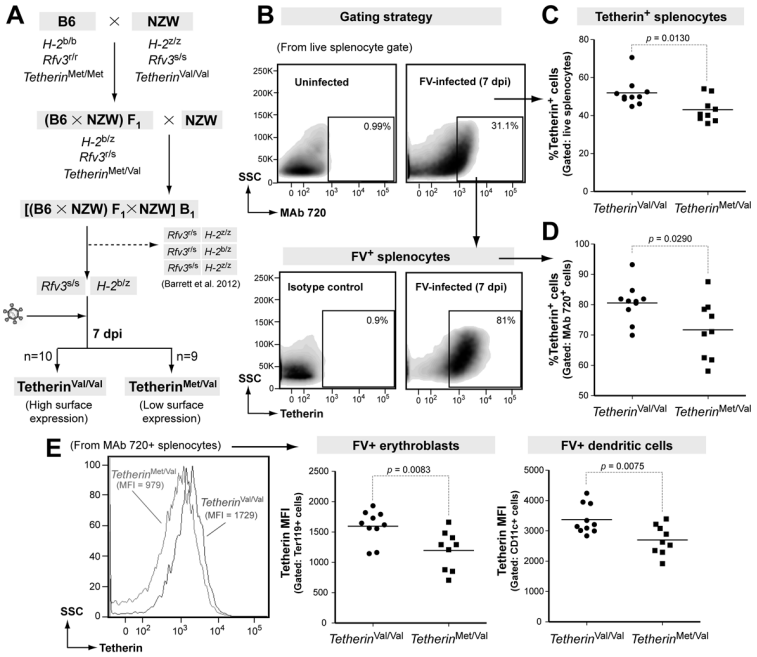

Figure 1. Lower Tetherin cell surface expression in *Tetherin*$^{Met/Val}$ B_1 mice

(**A**) Genetic backcrossing strategy. *Rfv3*$^{s/s}$ *H-2*$^{b/z}$ mice were genotyped as *Tetherin*$^{Val/Val}$ (endocytosis-defective, n=10) or *Tetherin*$^{Met/Val}$ (endocytosis-competent, n=9). B_1 mice were infected with 500 SFFU of NB-tropic FV/LDV and samples were analyzed at 7 dpi. (**B**) Gating strategy to quantify % Tetherin+ splenocytes. Tetherin+ cells were gated from an isotype control set at <1%. Note that the Tetherin+ population is not a distinct population. The MAb720+ population was also not a distinct population. The MAb720 gate were set using splenocytes of an uninfected mouse set at <1%. (**C**-**D**) Comparison of Tetherin+ splenocytes in *Tetherin*$^{Val/Val}$ versus *Tetherin*$^{Met/Val}$ B_1 mice. Tetherin expression were quantified in (**C**) total splenocytes and (**D**) FV-infected cells using the F-MuLV Env-specific MAb 720. (**E**) Tetherin mean fluorescence intensity levels, showing a histogram plot for total splenocytes and analyses for Ter119+ erythroblasts and CD11c+ DCs. Lines correspond to mean values and each dot corresponds to an individual mouse. Statistical analyses were performed using a 2-tailed Student's *t* test, with $p<0.05$ considered significant. Data were combined from 2 independent experiments.

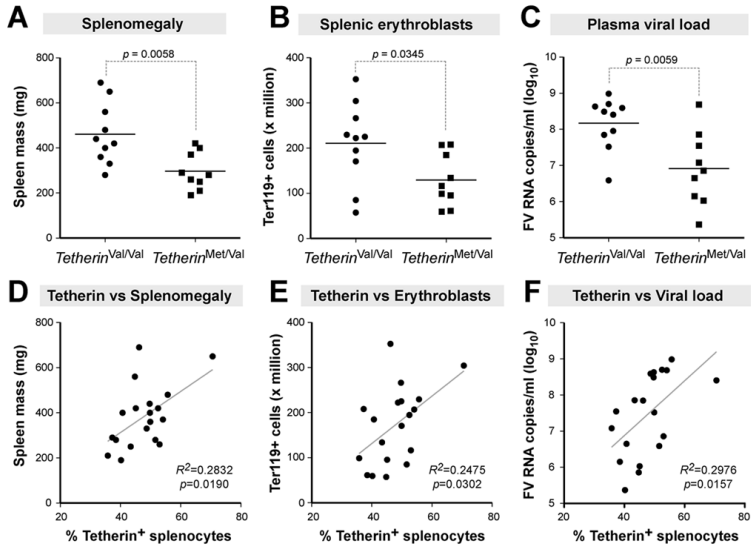

Figure 2. Endocytosis-competent Tetherin is associated with better control of acute FV replication and disease in *H-2*$^{b/z}$ B_1 mice

FV disease outcomes at 7 dpi in *H-2*$^{b/z}$ B_1 mice. (**A**) Spleen mass. (**B**) Absolute splenic erythroblast numbers. %Ter119+ cells obtained by flow cytometry were multiplied by the estimated total number of splenocytes based on the spleen mass, where 100 mg spleen was set at 10^8 cells. (**C**) Plasma viral load, based on qPCR for FMuLV RNA copies. Statistical analyses were performed using 2-tailed Student's *t* test. For panels A-C, the lines correspond to mean values. (**D-F**) Values from panels A to C were correlated against %Tetherin cell surface expression in the spleen, respectively. Best-fit linear regression lines with R^2 values are shown together with *p* values following Pearson product moment correlation analyses. For all panels, each dot corresponds to data from a single mouse. Data were combined from 2 independent experiments.

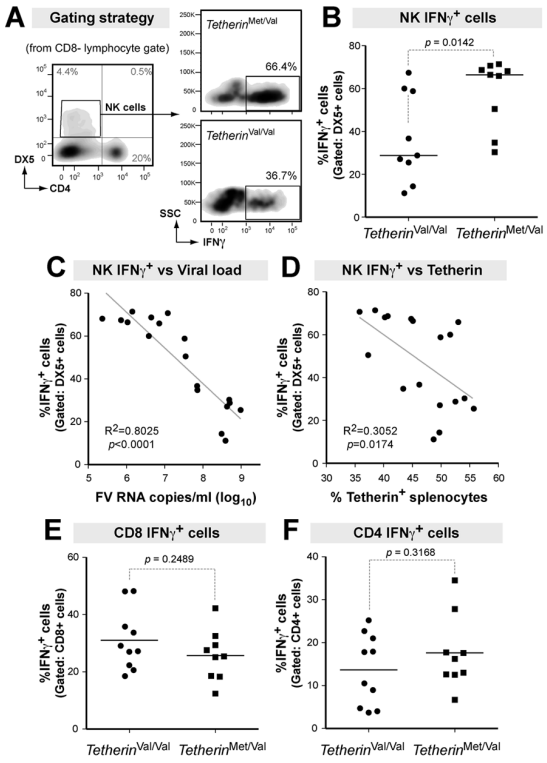

Figure 3. Endocytosis-competent Tetherin promotes stronger NK cell responses in *H-2*$^{b/z}$ B$_1$ mice

Splenocytes (7 dpi) were stimulated for 5 h with PMA/ionomycin prior to staining. (**A**) Gating strategy for quantifying intracellular IFNγ expression in DX5+ NK cells. Since DX5 can be expressed in some T cell subsets, the analyses focused on DX5+CD4-CD8- populations. (**B**) IFNγ+ + NK cells in the spleen. Correlation between IFNγ+ NK cells and (**C**) plasma viral load, and (**D**) %Tetherin surface expression in the spleen. (**E-F**) Comparison of 7 dpi intracellular IFNγ expression in splenic (**E**) CD8+ and (**F**) CD4+ T cells. For panels **B**, **E** and **F**, solid lines correspond to median values and each dot corresponds to data from a single mouse. Statistical analysis was performed using a 2-tailed Mann-Whitney U test. For panels **C** and **D**, best-fit linear regression lines with R^2 values are shown together with *p* values following Pearson product moment correlation analyses. Data were combined from 2 independent experiments.

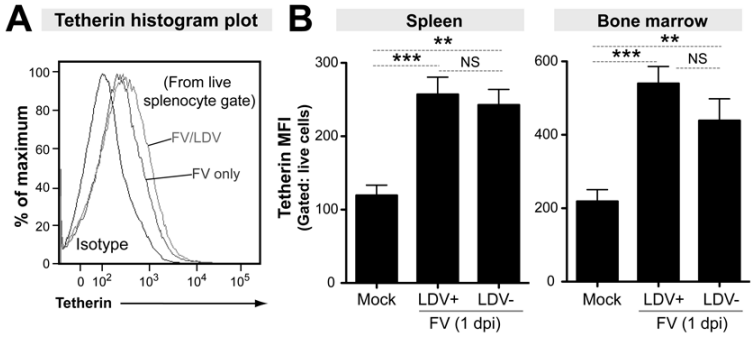

Figure 4. Tetherin cell surface expression is induced by FV independent of LDV co-infection

Spleen and bone marrow cells were harvested at 1 dpi following infection of B6 mice with mock (RPMI), 10^4 SFFU FV/LDV and 10^4 SFFU LDV-free FV (n=3 mice each). (**A**) Histogram plot from a live splenocyte gate showing Tetherin mean fluorescence intensity (MFI) relative to an isotype control. (**B**) Tetherin MFI values at 1 dpi. Bars correspond to mean values and error bars correspond standard deviations. Data were compared using a 2-tailed unpaired Student's *t* test. **, $p<0.01$; ***, $p<0.001$, NS, not significant ($p>0.05$).

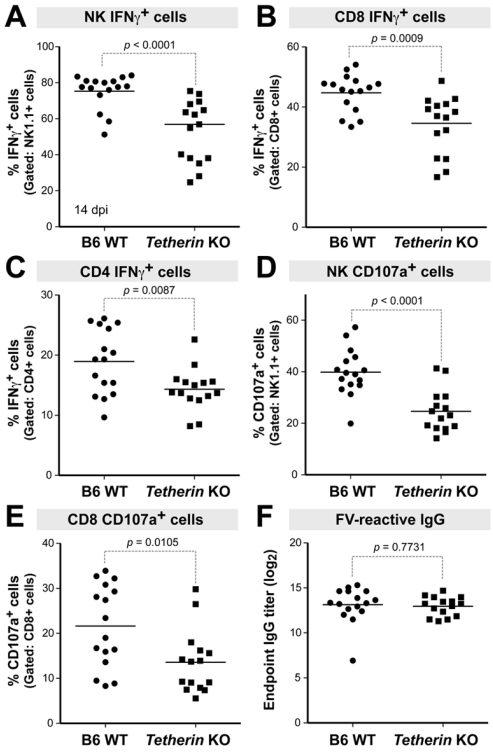

Figure 5. B6 Tetherin is associated with stronger cell-mediated immune responses to FV

Splenocytes harvested from B6 WT and B6 *Tetherin* KO mice at 14 dpi with 10^4 SFFU of LDV-free FV were stimulated with PMA/ionomycin for 5 h prior to staining for flow cytometry. (**A-C**) Intracellular IFNγ production in (**A**) NK1.1+ NK cells, (**B**) CD8+ T cells and (**C**) CD4+ T cells. (**D-E**) %CD107a expression in (**D**) NK cells and (**E**) CD8+ T cells. In panels **A** to **E**, B6 *Tetherin* KO mice had significantly lower cell-mediated immune responses. (**F**) Plasma FV-specific IgG endpoint titers as determined by ELISA. Statistical analyses were performed using a 2-tailed Student's *t* test. For all panels, lines correspond to mean values, and each dot corresponds to data from an individual mouse. Data were combined from 3 independent experiments.

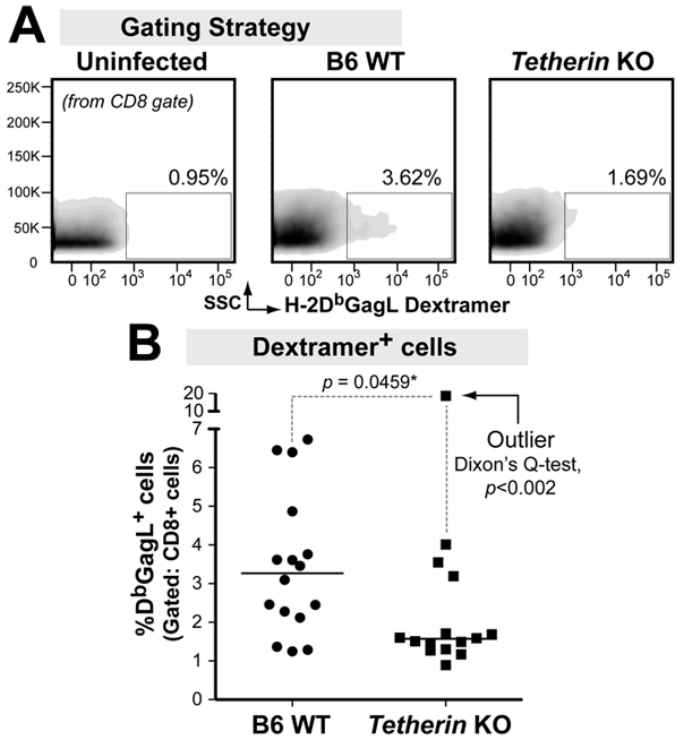

Figure 6. B6 Tetherin is associated with a stronger FV-specific CD8+ T cell response

(**A**) Gating strategy. Splenocytes from mice at 14 dpi were stained with anti-CD8 and a dextramer presenting the H-2D^b-restricted immunodominant GagL epitope. Note that the cells were not stimulated with PMA/Ionomycin. Gates were set against a stained uninfected sample. (**B**) Dextramer+ CD8+ T cells in the spleen. Lines correspond to median values and dots correspond to data from individual mice. Statistical analysis was performed using a 2-tailed Mann-Whitney U test. Dixon's Q test was used to confirm the statistical outlier in the *Tetherin* KO group. *Removal of the outlier adjusts the *p* value to 0.0150. Data were combined from 3 independent experiments.

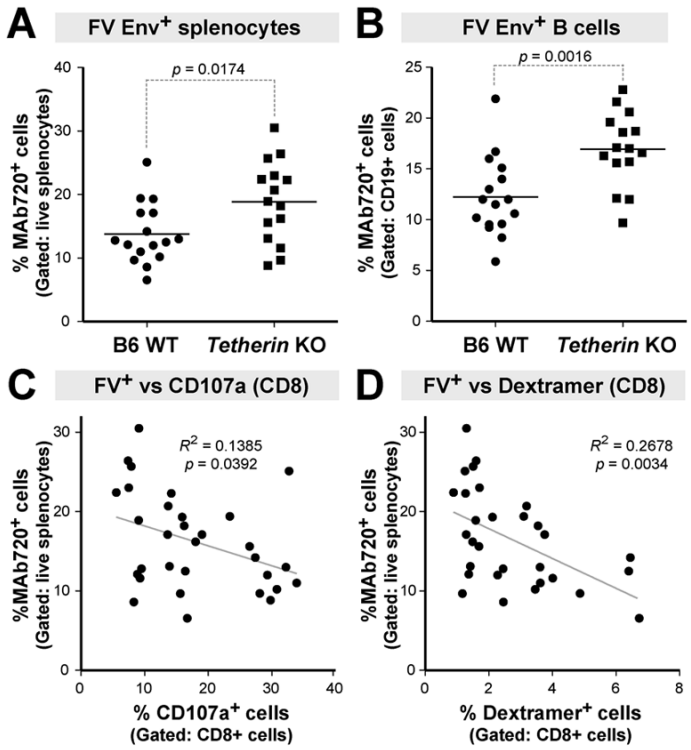

Figure 7. B6 Tetherin promotes immune control of cellular FV infection

Cellular FV infection levels in B6 WT and *Tetherin* KO mice at 14 dpi were quantified by flow cytometry using the F-MuLV Env-specific MAb 720 and specific cell subset markers. (**A-B**) Percentage of MAb 720+ in (**A**) total splenocytes and (**B**) splenic CD19+ B cells. Lines correspond to mean values and dots correspond to data from individual mice. Statistical analysis was performed using a 2-tailed Student's *t* test. (**C-D**) Correlation between MAb720+ splenocytes and (**C**) CD107a expression in CD8+ T cells and (**D**) %D^{b}GagL Dextramer+ CD8+ T cells. For panel **D**, the statistical outlier in the *Tetherin* KO cohort (Fig. 6B) was not included in the analysis. Best-fit linear regression lines with R^2 values are shown together with *p* values following Pearson product moment correlation analyses. Data were combined from 3 independent experiments.

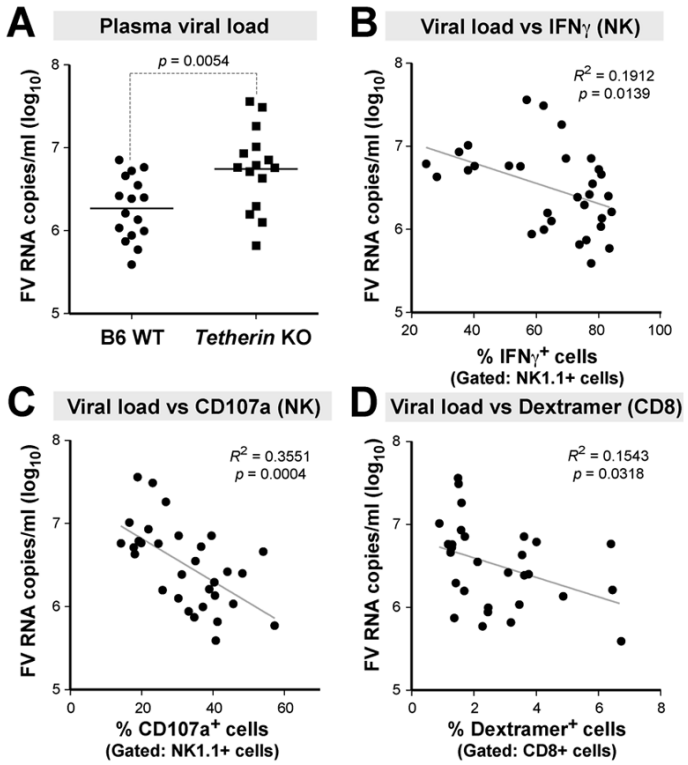

Figure 8. B6 Tetherin promotes immune control of FV plasma viremia

(**A**) Plasma viral loads from FV-infected B6 WT and *Tetherin* KO mice at 14 dpi were measured by qPCR and log-transformed prior to statistical analysis. Lines correspond to mean values and statistical analysis was performed using a 2-tailed Student's *t* test. Correlation between plasma viral loads and (**B**) %IFNγ+ NK cells, (**C**) %CD107a+ CD8+ T cells, and (**D**) %Dextramer+ CD8+ T cells. For panel **D**, the statistical outlier in the *Tetherin* KO cohort (Fig. 6B) was not included in the analysis. Best-fit linear regression lines with R^2 values are shown together with *p* values following Pearson product moment correlation analyses. Data were combined from 3 independent experiments.